LAWRENCE
LIVERMORE
NATIONAL
LABORATORY

UCRL-TR-211363

Validation of Air-Backed Underwater Explosion Experiments with ALE3D

Lara D. Leininger

April 14, 2005

This work was performed under the auspices of the U.S. Department of Energy by University of California, Lawrence Livermore National Laboratory under Contract W-7405-Eng-48.

UCRL-TR-316226

VALIDATION OF AIR-BACKED UNDERWATER EXPLOSION EXPERIMENTS WITH ALE3D

Lara D. Leininger

Defense Systems Analysis Group, Engineering
Missiles and Nuclear Technology Section, NAI
Lawrence Livermore National Laboratory
Livermore, California, 94551

March 21, 2005

Work performed under the auspices of the Department of Energy by the Lawrence Livermore National Laboratory under Contract W-7405-Eng-48.

DISCLAIMER

ABSTRACT

This paper summarizes an exercise carried out to validate the process of implementing LLNL's ALE3D to predict the permanent deformation and rupture of an air-backed steel plate subjected to underwater shock.

Experiments were performed in a shock tank at the Naval Science and Technology Laboratory in Visakhapatnam India, and the results are documented in reference [1] (Ramajeyathilagam, 2004). A consistent set of air-backed plates is subjected to shocks from increasing weights of explosives ranging from 10g-80g. At 40g and above, rupture is recorded in the experiment and, without fracture mechanics implemented in ALE3D, only the cases of 10g, 20g, and 30g are presented here.

This methodology applies the Jones-Wilkins-Lee (JWL) Equation of State (EOS) to predict the pressure of the expanding detonation products, the Gruneisein EOS for water under highly dynamic compressible flow - both on 1-point integrated 3-d continuum elements. The steel plates apply a bilinear elastic-plastic response with failure and are simulated with 3-point integrated shell elements. The failure for this exercise is based on effective (or equivalent) plastic strain.

1.0 INTRODUCTION AND BACKGROUND

Recent terrorist activities have brought attention to the vulnerability of the US infrastructure to underwater explosions. Scientists and engineers have been executing experiments and validating those experiments for decades and the literature has numerous examples of air-backed underwater explosions on sheet metal, as well as fewer experiments on the air-shocked sheet metal.

In general, the numerical simulations in the literature for validation with experiment employ a decoupled approach that begins with analytically attained approximations of the expected pressure time-history on the plate that is applied as a boundary condition to a finite element method with a 2-d Lagrangian shell element formulation. The de-coupled approach assumes that the shock is hitting a rigid (non-deforming) structure, thereby ignoring the shock energy absorbed in plastic deformation of the structure. This leads to a higher expected pressure pulse, and a conservatively large deformation.

There is added value to achieve a fully-coupled 3-d simulation that includes the significant effects of fluid-structure interaction and is flexible enough to account for multiple explosives, transmission media, and structures. This paper summarizes the first step: a validation of a particular case (plastic explosive, underwater, against steel).

Although the simulation is fully coupled the "main events" of the simulation can be interchanged to account for differences in situation (*i.e.* a new EOS can be substituted to account for an Improvised Explosive Device, IED, or the parameters of the deviatoric response can be altered to account for aluminum or concrete). Future developments should also account for the non-continuum fracture response of the structure.

2.0 COMPUTATIONAL MODEL

The computational models used for this exercise assume that the explosive products expansion can be modeled using the Jones-Wilkins-Lee EOS for C-4, the shock propagation through water is modeled using a Gruneisen EOS, and the deviatoric/strength response is modeled by a J2 flow elastic-plastic bilinear curve with failure. The convenient units for the high pressures and length scale of this problem are centimeter [cm], gram [g], microsecond [μs], megabar [Mbar], and Kelvin [K].

2.1 JONES-WILKINS-LEE EQUATION OF STATE FOR EXPLOSIVES

The Jones-Wilkins-Lee (JWL) equation of state predicts the pressure-volume response of expanding detonation products at times after an explosion. This EOS approximates the energy release of the explosive in a shape independent way and assumes that all the energy released from the explosive spontaneously becomes expanding detonation products. This is often referred to as a volumetric burn model as opposed to an exact "burn" model that takes into account the shock front burning though the explosive. This can be a source of inaccuracy within the model. The JWL EOS takes the form (ALE3D manual, 2003):

$$P = A\left(1-\frac{\omega}{R_1 v}\right)e^{-R_1 v} + B\left(1-\frac{\omega}{R_2 v}\right)e^{-R_2 v} + \frac{\omega E}{v}$$

where A B, R_1, R_2, and ω are material constants, and v and E are the relative volume and internal energy of the material respectively. The material constants are determined by measuring the pressure on the case of cylindrically shaped explosives. Scaling of these parameters for the spherical explosive found in this experiment could be another source of uncertainty.

Furthermore, the source in this experiment is an Indian explosive named PEK-1, which is described as a plastic explosive with an energy 1.17 times that of TNT (Ramajeyathilagam, 2004). With little else to go on, the parameters of Composition-4 (C4) – a plasticized RDX (Research Development Explosive) with an energy density 1.2 times that of TNT – is used to describe PEK-1 at the ranges of explosive weight for this experiment. This assumption could cause the computed answer to diverge at larger weights where the energetics of C4 surpass those of PEK-1 (given what little we know about PEK-1).

2.2 Gruniesen Equation of State for Water

For the treatment of compressible fluid propagating the detonation shockwave, the Gruneisen Equation of State (EOS) is used within the framework of ALE3D. Explosive detonation and shock response of water is unlike that through air. Experiments have shown that there is a strong peak overpressure followed by a second peak from shock reflections within the boundaries of the detonating explosive (Cole, 1948). There is also a third peak at longer timescales as a result of vaporization of water under negative pressure that is termed cavitation. Theoretical derivations of the shock time history that are usually found in the literature as boundary conditions to a structural response calculations, correctly predict the impulse of the incoming shockwave, and these time histories take the form of exponential decay. The Gruneisen EOS has a cubic polynomial form that captures unique behavior of the second peak (not found in an exponential). The Gruneisen EOS takes the form (DYNA3D Manual/Woodruff, 1973):

$$P = \frac{\rho_O C^2 \mu [1 + \mu (1 - \frac{\gamma_O}{2}) - \frac{a\mu^2}{2}]}{[1 - \mu (S_1 - 1) - \frac{S_2 \mu^2}{\mu + 1} - \frac{S_3 \mu^3}{(\mu + 1)^2}]^2} + E(\gamma_O + a\mu) \text{ for: } \mu > 0 \text{ (compression)}$$

$$P = \rho_O C^2 \mu + E(\gamma_O + a\mu) \text{ for: } \mu < 0 \text{ (expansion)}$$

$$\mu = \frac{1 - v}{v}$$

where C, S_1, S_2, S_3, γ_o, and a are material constants, and ρ_o, v, and E are the initial density, relative volume, and internal energy of the material respectively. Two different parameter sets to populate this EOS were found in the literature, and those two sets are used to create the pressure-volume response curves shown in Figure 1. The first set comes from a paper that documents a thorough validation of parameters for water based on analytical and experimental results (Molyneaux, et. al, 1994), and the second set of parameters come from a database used widely at Lawrence Livermore National Laboratory (LLNL).

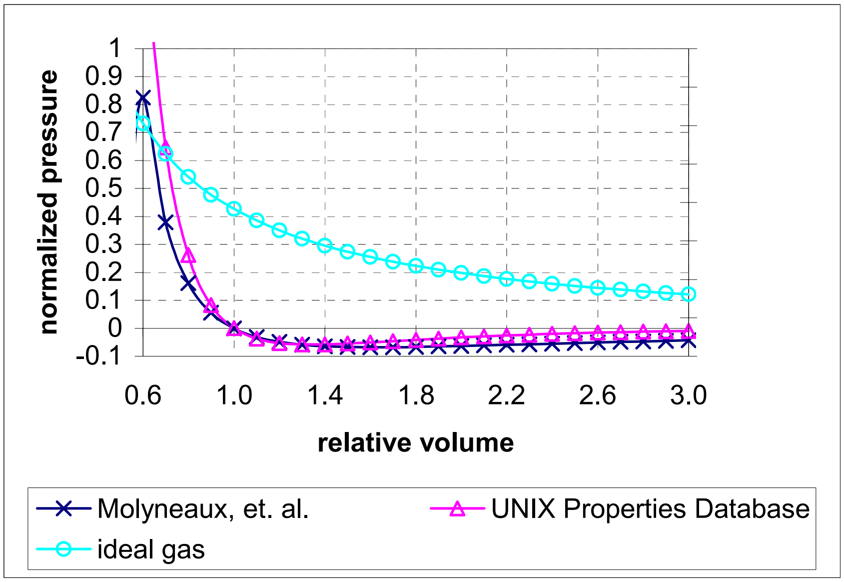

Figure 1: Comparison of different material constants in the Gruneisen Equation of State

It can be seen in the graph of the EOS for these parameters that the pressure response does not vary significantly for the two cases, and that the physics dictate that there will be a positive pressure response in compression ($v < 1$) and a negative pressure response in expansion ($v > 1$). For comparison, the ideal gas equation of state pressure volume response is also included in Figure 1, and shows that there is no negative pressure response for shocks in air.

The PV response in Figure 1 is only valid for liquid water in the range $0.6 < v < 3$. At high compression and expansion, there are phase changes in water that are not accounted for in this model. Furthermore, water is a material that cannot handle tension from negative pressure. In fact, the literature suggests that the maximum negative pressure that could be sustained by water is one atmosphere (1e-6 Mbar) but is most likely zero (Cole, 1948; Clutter, 2004; Driels, 1980). This physical behavior commands that the pressure in the EOS must be "cut-off" at a reasonable value. Parameter studies in ALE3D indicate that there is no difference between the structural response when the cut-off is set to 0 or 1e-6Mbar, so the cut-off is set to 0 atm to be consistent with the literature.

There have been studies in the literature (Driels, 1980) that look further into the assumption that there could be a significant negative pressure response in water. The reasoning for this argument suggests that the gas content of water causes water to "break" at effectively zero atmospheric pressure. Therefore if the water could be degassed, by either excessive hydrostatic pressure or from the dynamic pressure of another shock, then the water could sustain higher levels of negative pressure without cavitating. These findings are not applicable for this study because the depth of the charge is only 2 m, resulting in a hydrostatic pressure of less than 3 psi and there is no previous shock exposure.

2.3 DEVIATORIC RESPONSE FOR STEEL

The deviatoric (or strength) model of steel is modeled using an elastic-plastic response with a bilinear yield curve and effective plastic strain yield criterion. The Belytschko-Tsay shell element formulation is implemented with 3 integration points through the thickness. The parameters for the steel plate come directly from Ref. [1].

The advantage of using the shell element formulation over 3-d continuum solid elements is that dividing a thin plate (0.2 cm thickness) into a significant number of one-point integrated solid elements will be Courant limiting to the point that a fully-coupled fluid-structure interaction solution could not be computed. Conversely, although the bending response of a single shell element is superior to that of a solid element, the shear response is not necessarily accurately represented. For the response of the plate for these experiments the bending response will dominate in the center of the clamped plate, but the shear response will dominate at the constraints. This develops uncertainty if the majority of the effective plastic strain (and rupture) is found at the boundaries.

3.0 NUMERICAL CONVERGENCE

To check for numerical convergence of the fluid model, 4 computational cases (without the structure) were run, varying the ranges of mesh density. For each of these cases, the pressure time history and impulse are compared at a standoff of 25 cm. The results for this convergence study are shown in Figure 2. Table 1 shows the impact of the computational burden for the increasing resolutions. It is important to note that the medium range of mesh resolution calculated an impulse that is only 4% off the value that was calculated for the finest case, while consuming only 18% of the computational resources that are required for that finest mesh resolution. Furthermore, these convergence tests are on a length scale much smaller than the real problem. When the actual problem is generated using the medium mesh resolution, the continuum element count goes up to 1.2M zones. If the finest resolution were used, the problem would be on the order of 13M zones – which is a challenge to run, even with our computational resources, and definitely not feasible for a parameter study.

Considering the balance between computational resources and accuracy, it is determined that the ideal the mesh density for this exercise is the medium case.

Table 1: Comparison of computational effort for the numerical convergence studies

case	No. of continuum elements	Run time	No. of processors	Peak Overpressure [Mbar]	Impulse [Mbar-μsec]
Coarse	88,000	3 min	10	3.54e-4	0.445
Medium	648,000	15 min	10	5.73e-4	0.603
Fine	5,585,000	52 min	10	6.99e-4	0.606
Finest	7,036,000	1 hr 24 min	50	8.02 e-4	0.627

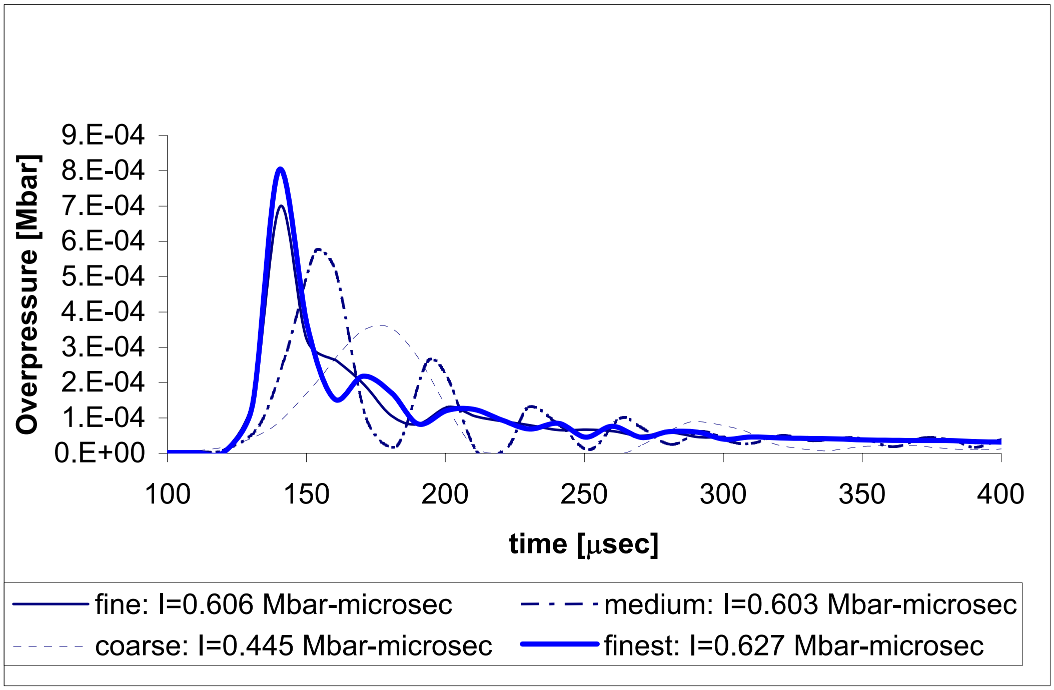

Figure 2: Mesh resolution cases for numerical convergence

4.0 ALE3D RESULTS

Figure 3 shows the finite element model used for the calculations in this exercise. The computed results are summarized in Table 2 and are also shown in Figures 4, 5, and 6 for the 10g, 20g, and 30g cases respectively.

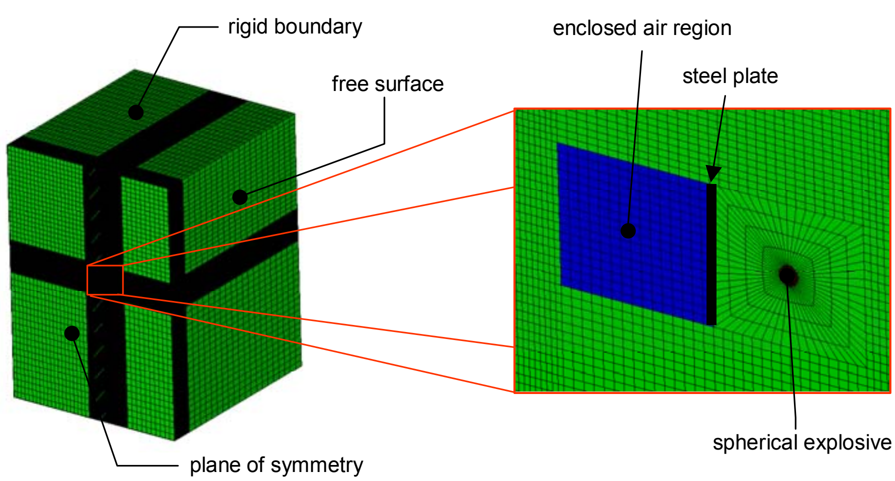

Figure 3: Finite Element Mesh used for exercise

As described in Section 2.1, the computational model uses an equation of state for the detonation products that is expected to predict larger plate deformation than the explosive used in the experiment. Furthermore, because of the non-linear nature of the volumetric burn EOS, this disparity between experiment and computation should grow larger as the weight of the explosive increases. Table 2 summarizes the computed displacements using the weight of PEK-1 as the input weight of C-4. As expected, the computed displacement diverges significantly at the highest weight.

Table 2: Comparison of computed and experimental obtained displacement at the center of the plate

Weight of PEK-1 [g]	Equivalent weight of C-4 [g]	Computed displacement [cm]	Experimental displacement [cm]
10	10	3.9	4.00
20	20	6.3	5.78
30	30	8.6	6.77

To evaluate the relationship between the weight of PEK-1 used in the experiment and the equivalent weight of higher energy C-4 that should be used in this exercise, a series of calculations were performed at various weights of C-4 and the resulting permanent deformations were recorded. The recorded displacements from the C-4 calculations are correlated to the displacements documented in the experiment, and an equivalent weight of C-4 for each PEK-1 case is determined. Figure 4 shows the data points from this computational excursion, and the resulting linear relationship between the weight of PEK-1 and the equivalent weight of C-4.

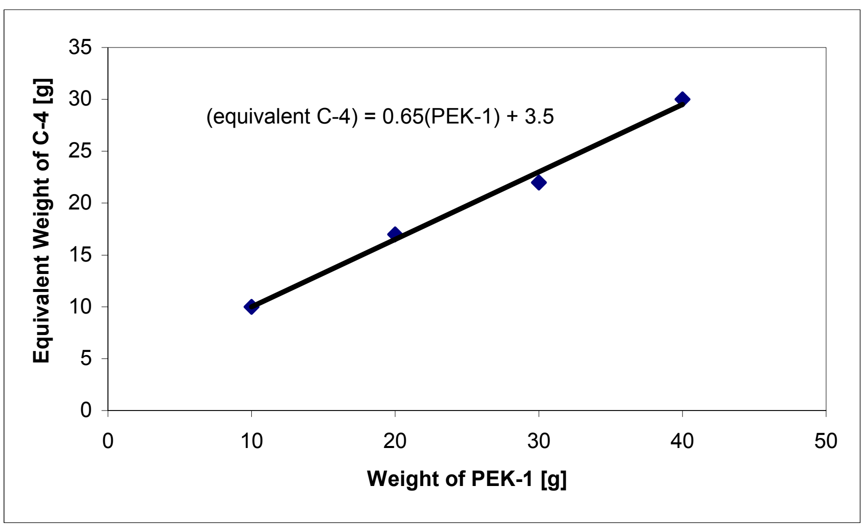

Figure 4: Linear relationship to determine equivalent weight of C-4 used in calculation (derived based on the structural deformation of the steel plate)

The aforementioned linear relationship reduces the input weight of the C-4 in the computational model. The scaling enables good agreement with experimental data, as shown in Table 3. Figures 4, 5, and 6 show detailed time histories for the scaled models.

Table 3: Comparison of computed and experimental obtained displacement at the center of the plate

Weight of PEK-1 [g]	Equivalent weight of C-4 [g]	Computed displacement [cm]	Experimental displacement [cm]
10	10	3.9	4.00
20	17	5.7	5.78
30	22	6.6	6.77

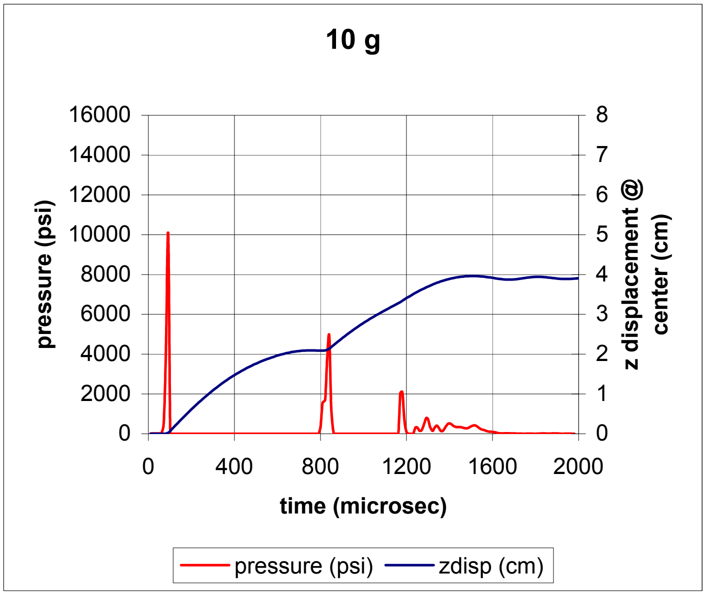

Figure 4: Pressure and displacement time history at the center of the plate

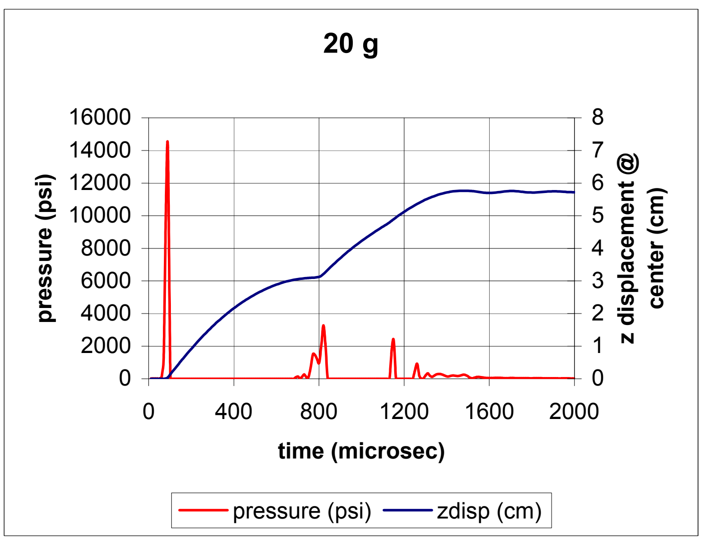

Figure 5: Pressure and displacement time history at the center of the plate

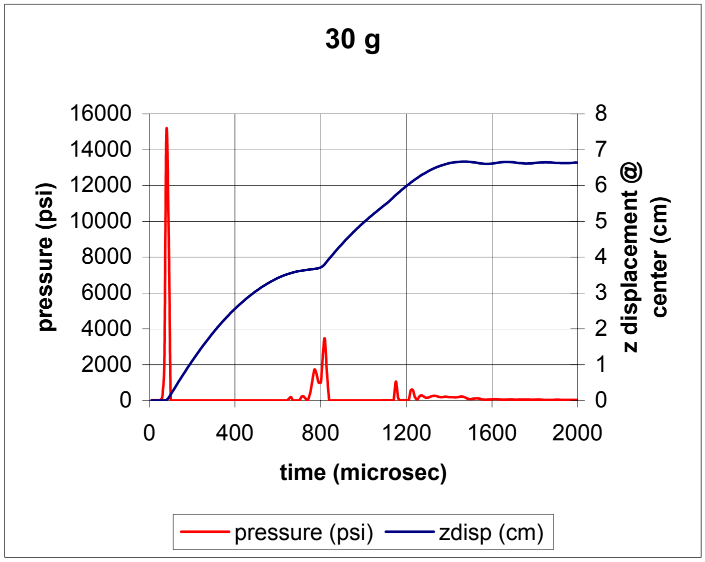

Figure 6: Pressure and displacement time history at the center of the plate

In addition to recording the magnitude of permanent deformation, the plates were inspected for visual cues that there would be rupture. For the 10g, 20g, and 30g cases, there were no indicators of rupture observed in the experiment. Figures 7, 8, and 9 show fringe plots of the computed effective plastic strain in the plates for the cases of 10g, 20g, and 30g of explosive all at 2 ms (2000 μsec). The range of the fringe is 0% (blue) to 36% (red) effective plastic strain. As shown in the figures, no part of the steel plate has exceeded 36% effective plastic strain - which is the strain at rupture for this alloy (Ramajeyathilagam, 2004*)*. The experimental data showed no evidence of rupture in the plates, and this computation is consistent with that data.

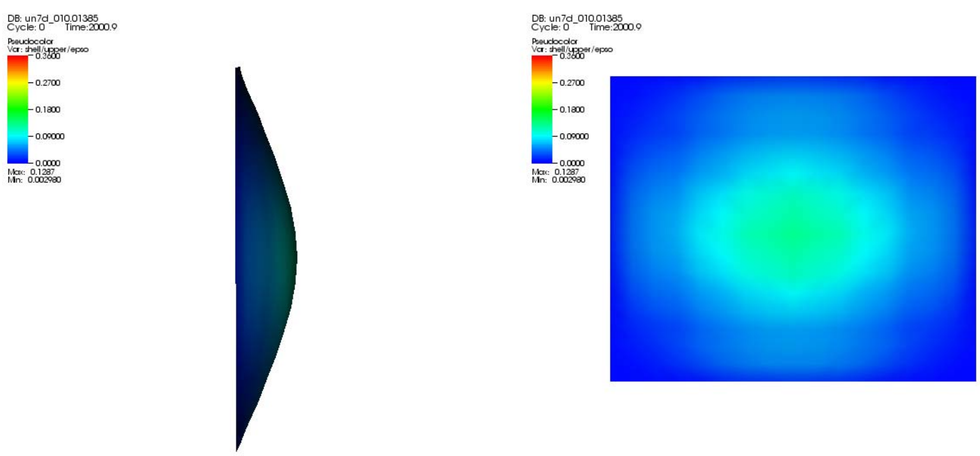

Figure 7: Computed fringe plot of effective plastic strain in the plate

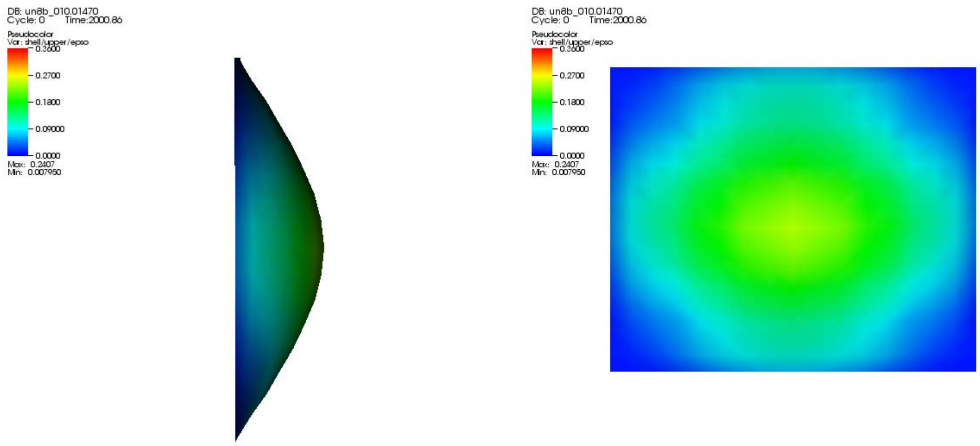

Figure 8: Computed fringe plot of effective plastic strain in the plate

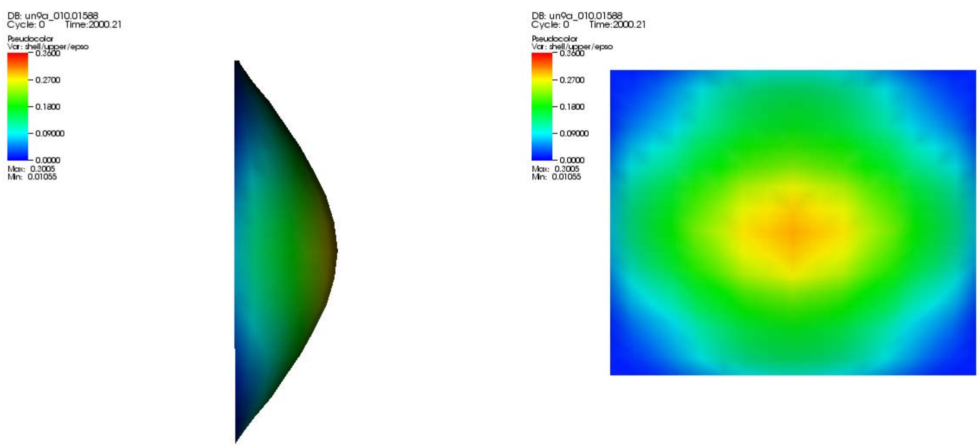

Figure 9: Computed fringe plot of effective plastic strain in the plate

5.0 CONCLUSIONS

Presented here is an exercise carried out to validate (with an experiment out of the literature) the process of implementing LLNL's ALE3D to predict the permanent deformation and rupture for an air-backed steel plate subjected to underwater shock. A computational model is built using the Jones-Wilkins-Lee equation of state (EOS) for the pressure-volume response of detonation products, the Gruneisen EOS for propagation of shock underwater, and a bilinear elastic-plastic curve with failure for the deviatoric response of a steel plate.

There was no available equation of state data for the explosive used in experiment, so properties were assumed based on the properties of a known plastic explosive. Initial results from the computation show that the computed magnitude of plastic deformation diverges from the experimentally obtained values, and that this divergence worsens as the explosive weight increases. It can be concluded that the results are sensitive to the energetics of the explosive and that the exponential terms in the JWL EOS influence this sensitivity and subsequent divergence. In this paper, a linear relationship is used to reduce the equivalent input weights for the calculations and this leads to good agreement with experimental data.

These computations clearly demonstrate the capability of computing fully-coupled, fluid-structure, interaction problems with LLNL's ALE3D, specifically for the structural response of underwater explosions. Although it remains to be demonstrated, it is assumed that this process can be implemented to robustly predict the response of any thin-walled structure to blast loading.

6.0 REFERENCES

[1] Ramajeyathilagam, K. and C. P. Vendhan, "Deformation and rupture of thin rectangular plates subjected to underwater shock", International Journal of Impact Engineering, Vol. 30, pp.699-719, (2004).

[2] Anderson, A. et. al. "User Manual for ALE3D, An arbitrary Lagrange Eulerian System, Version 3.4" Lawrence Livermore National Laboratory, January 31, 2003.

[3] Cole, R. H., Underwater Explosions, Princeton University Press, 1948.

[4] Whirley, R.G. and B. E. Engelmann, "DYNA3D User Manual", UCRL-MA-107254, November 1993.

[5] Molyneaux, T. C., L. Li, and N. Firth, "Numerical Simulations of Underwater Explosions", Computers Fluids Vol. 23, No. 7, PP. 903-911 (1994).

[6] Clutter, J. K., and M. Stahl, "Hydrocode simulations of air and water shocks for facility vulnerability assessments", Journal of Hazardous Materials, vol. 9, no. 24, pp. 9-24, (2004).

[7] Driels, M. R., "The effect of a non-zero cavitation tension on the damage sustained by a target plate subject to an underwater explosion" Journal of Sound and Vibration, vol. 73, no. 4, pp. 533-545, (1980).